Macromolecules **2003,** *36,* 5661−5665

Mechanism of Decay Reaction of Free Radicals Trapped in Poly(tetrafluoroethylene) Related with the Heterogeneity in Structure

Shigero Hara,[†] Katsuhiro Yamamoto,[†] Shigetaka Shimada,*[,†] and Hajime Nishi[‡]

Nagoya Institute of Technology, Gokiso-cho, Showa-ku, Nagoya 466-8555, Japan, and Hitachi Cable Ltd., 5-1-1, Hidaka-cho Hitachi 319-1414, Japan

Received April 7, 2003

ABSTRACT: Reactions of free radicals produced in γ-irradiated poly(tetrafluoroethylene) (PTFE) were studied by electron spin resonance spectroscopy. β-Scission reaction of main chain radicals and fluorine abstraction of chain end radicals were detected directly. The decay reactions of the free radicals were examined in connection with molecular motion of the matrix polymer. The rates of those reactions were also discussed in relation to much heterogeneity in structure. Behaviors of free radicals trapped in cross-linked PTFE were compared with those in non-cross-linked PTFE to clarify the effects of molecular motion and structure on the reactions in the solid state.

1. Introduction

Shimada et al.[1−6] related chemical reaction of free radicals trapped in solid polymers closely with molecular motion and physical structures of the polymers such as molecular orientation. The decay reaction was interpreted in terms of diffusion-controlled process of the free radicals and various heterogeneity such as the distribution of relaxation time and the molecular disorder of a polymer chain in crystalline and noncrystalline regions. Other authors[7−9] studied diffusion-controlled process of oxygen molecules to formation of peroxy radicals. In the present article, we study the decay reaction of free radicals trapped in poly(tetrafluoroethylene) (PTFE). The decay should contain several reactions.

For example, the free radical migration in the polymer matrices is indispensable for the decay reaction in the crystalline and paracrystalline regions below the melting temperature because of the inhibition of translation diffusion of the segments. The free radical migration is the repetitions of fluorine atom abstraction of the polymer radicals from the other segments. Many authors[10−15] studied the free radicals produced in γ-irradiated PTFE by electron spin resonance spectroscopy. Main chain radical, $-CF_2(\beta)-C^{\bullet}F(\alpha)-CF_2(\beta)-$ ($M^{\bullet}$), chain end type radical, $-CF_2(\beta)-CF_2{}^{\bullet}(\alpha)$ ($E^{\bullet}$), and their peroxy radicals are clearly detected. Siegel et al.[16] observed the conversion of main chain peroxy radical, $-CF_2(\beta)-C(OO^{\bullet})F(\alpha)-CF_2(\beta)-$, to $E^{\bullet}$ by UV illumination in a vacuum. The heterogeneity in the PTFE solid includes also some twisted helix structures in the crystalline, paracrystalline, and noncrystalline regions.

In the present study, we clarify the mechanism of the decay reaction of the free radicals related with the heterogeneity in the solid state. We use also the cross-linked PTFE which has a low crystallinity and many cross-links in the noncrystalline region. The radiation-induced cross-linking of PTFE was performed by irradiation around 613 K by Tutiya,[17] Sun et al.,[18] and Tabata et al.[19−21] to improve the yield strength and Young's modulus in mechanical properties, radiation resistance, and light transparency. Oshima et al.[22,23] compared free radicals trapped in the cross-linked PTFE and their reactivity with them in the non-cross-linked one. The difference between the cross-linked and non-cross-linked PTFE helps the confirmation of the mechanism of the decay reaction. These studies should give a great contribution to the mechanism of deterioration and relaxation phenomena of PTFE solid as well as graft copolymerization for the modification of PTFE in the solid state.

2. Experimental Section

Materials. A cross-linked PTFE film (XF-2 ca. 500 μm in thickness) was obtained from Hitachi Cable Co. Ltd., and a non-cross-linked PTFE powder sample was Fluon G163 (product of Asahi Glass Co. Ltd.). The cross-linked and non-cross-linked samples are called CL and NCL PTFE, respectively.

Irradiation Techniques. All samples were subjected to γ-irradiation by the use of ^{60}Co γ-ray source (Mitsubishi Denki Co. Ltd.) at room temperature under a vacuum of 10^{-4} Torr at the dose rate of ca. 0.2 kGy/h. The total doses for the CL and NCL samples are ca. 30 and 70 kGy, respectively. The concentrations of free radicals produced in the CL and NCL samples are also 3.5 and 1.2×10^{18} spins/g, respectively. The samples have the same order of magnitude of free radicals. Then, all chemical reactions observed in the present study should be related with each other, as mentioned later. A sample was subjected to UV irradiation in a vacuum to conversion of main chain peroxy radicals to chain end radicals ($E^{\bullet}$) of PTFE. The UV irradiation was carried out with a HLS-4002BV mercury vapor lamp (Toshiba Denki Co. Ltd.).

ESR Measurements. ESR spectra were observed at a low microwave power level to avoid power saturation and with 100 kHz modulation using JEOL FE3XG spectrometers (X-band) at room temperature coupled to a microcomputer (NEC PC-9801). The PTFE sample was placed in a Spectrosil sample tube, which was connected to a vacuum line and degassed. The signal of DPPH (1,1-diphenyl-2-picrylhydrazyl) was used as a g-value standard. The magnetic field was calibrated with the well-known splitting constants on Mn^{2+} in MgO.

3. Results and Discussion

Free Radicals Produced by γ-Irradiation. Figure 1 shows ESR spectra of free radicals produced in irradiated NCL (a) and CL (b) PTFE measured at room temperature. The γ-irradiation was carried out at room temperature. The unstable free radicals have already disappeared because of low T_g of PTFE (ca. −30 °C).

[†] Nagoya Institute of Technology.

[‡] Hitachi Cable Ltd.

* Corresponding author: e-mail shimada@mse.nitech.ac.jp.

10.1021/ma030206v CCC: $25.00

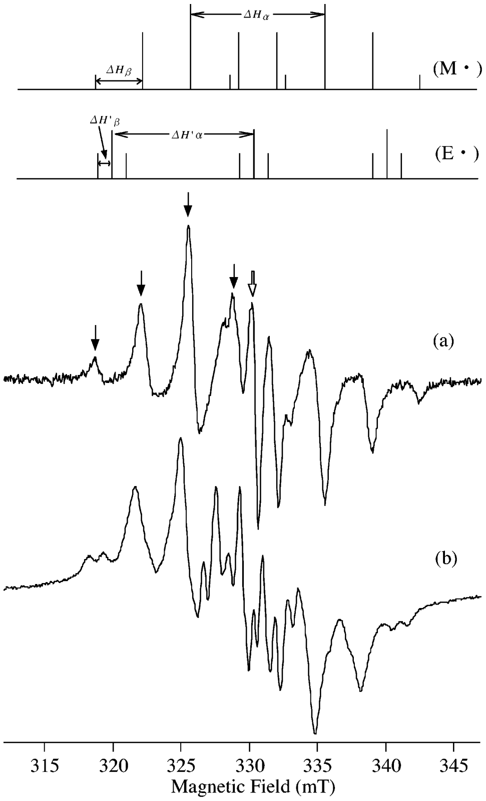

Figure 1. ESR spectra of γ-irradiated NCL (a) and CL (b) PTFE measured at room temperature. The γ-irradiation was carried out at room temperature. The characteristic peaks indicated by arrows are originated from the main chain alkyl type (M$^\bullet$) (filled arrows) and chain end alkyl type (E$^\bullet$) (open arrow) radicals. The stick diagrams of the ESR spectra are depicted for the understanding of the assignment. The heights of the sticks represent the relative intensities of the lines.

The spectra are composed of the double quintet (2×5 lines) and triple triplet (3×3 lines), which are observed by some authors.[10−16] The low intensity of the triplet spectrum was associated with chain end type free radicals, $-CF_2(\beta)-CF_2^\bullet(\alpha)$ (E$^\bullet$).The spectra of the 2×5 lines were assigned to those of chain alkyl free radicals, $-CF_2(\beta)-C^\bullet F(\alpha)-CF_2(\beta)-$ (M$^\bullet$). Those assignments are based on the analyses of hyperfine splitting (hfs) caused by the interaction between the unpaired electron and fluorine nucleus. The 2×5 lines were produced from five F atoms ($I = {}^1/_2$): four equivalent F(β) (coupling constant, $\Delta H_\beta \cong 3.3$ mT) and one different F(α) (coupling constant, $\Delta H_\alpha \cong 9.0$ mT). The 3×3 lines were also produced from two F(α) atoms of a large hfs (coupling constant, $\Delta H'_\alpha \cong 17$ mT) and two F(β) of a small hfs (coupling constant, $\Delta H'_\beta \cong 1.6$ mT). Tamura[12] studied the temperature dependence of ESR spectra for the irradiated PTFE. The spectrum at 300 K observed by him is sharp and similar to those in Figure 1a. The stick diagrams are also depicted in the figure. Oshima et al.[22,23] have already studied free radicals trapped in cross-linked PTFE and compared its behaviors with those in non-cross-linked PTFE. They observed a broad singlet spectrum from alkyl type radicals trapped in the cross-linked region and much higher *G* value (radiation yield) of radicals in the cross-linked sample than the non-cross-linked sample. The broad singlet cannot be detected clearly in CL PTFE as shown in Figure 1b because of the low cross-linking density, though ca. 8 times higher *G* value of radicals in the CL PTFE in the present study. Oshima et al.[22] stated that the high *G* value in cross-linked PTFE may be due to a selective energy or charge transfer to the cross-linking site from the initial highly excited states or a role of subexcited electrons.

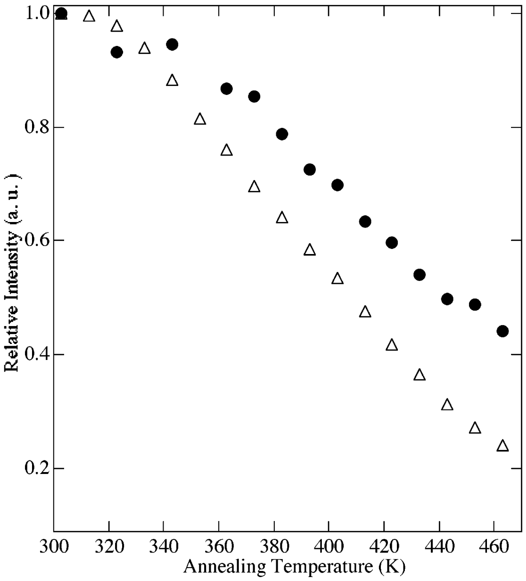

Figure 2. Decay curves of the free radicals in γ-irradiated NCL (●) and CL (△) PTFE (change of radical concentration with temperature of heat treatment).

The relative intensity of the triplet spectrum due to E$^\bullet$ in CL PTFE is stronger than that in NCL PTFE. This is caused by the low crystallinity in CL PTFE. For instance, the probability of back-reaction of E$^\bullet$ produced by scission of polymer chain, $E^\bullet + E^\bullet \rightarrow E-E$, is much lower in noncrystalline and disordered regions than in crystalline region. The low probability of the back-reaction may be one of the reasons of high *G* value in the cross-linked PTFE.

Decay Reaction of Free Radicals. Figure 2 shows decay curves of free radicals by the following procedure. The ESR spectrum was observed at room temperature after γ-irradiation. Next, the sample was heated and stored at a high temperature for 5 min and then cooled to room temperature at which the ESR spectrum was again observed. The same heat treatment was applied with successively increasing temperatures. The relative intensities of the spectra after each heat treatment was plotted against the temperature of heat treatment. The free radicals in NCL PTFE begin to decay around 350 K. The decay region falls in the range of molecular relaxation in paracrystalline PTFE associated with the so-called α-dispersion observed in mechanical studies. This fact suggested that the decay of free radicals is closely related with molecular motion in the paracrystalline region. On the other hand, free radicals in CL PTFE starts to decay around 330 K lower than 350 K in NCL PTFE. This difference may be caused by more disordered structure of the paracrystalline region in CL PTFE, formed by many cross-links. To confirm the relation between the decay reaction and molecular motion of PTFE, the variation of the concentration of free radicals was measured as a function of the duration of storage time at several temperatures, as shown in Figure 3. The following results are found. (a) The decay rates of the free radicals in more disordered region of CL PTFE are larger than in NCL PTFE, as expected. (b) A fractional amount of free radicals cannot decay at temperatures of heat treatment. The fractional amount

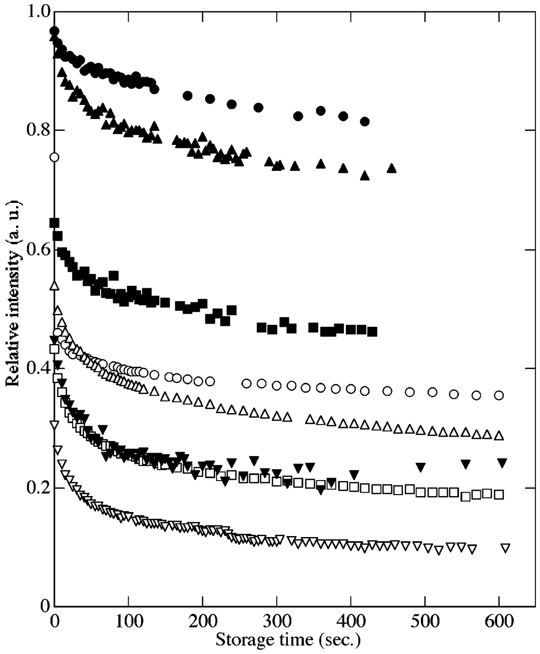

Figure 3. Decay curves of the free radicals in γ-irradiated NCL (closed symbols) and CL (open symbols) PTFE at 373 K (●, ○), 403 K (▲, △), 433 K (■, □), and 453 K (▼, ▽) (change of radical concentration with storage time at various temperatures).

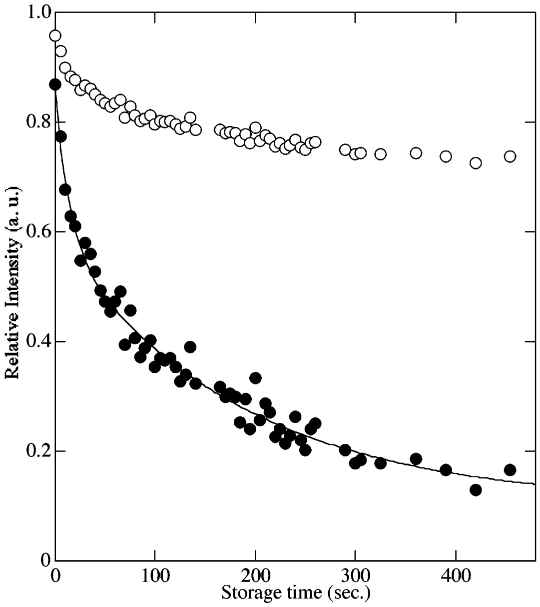

Figure 4. Decay curves of the free radicals in γ-irradiated NCL PTFE at 403 K. Open symbols are experimental. Closed symbols are the reduced fractional amounts of free radicals, calculated by subtracting the spectral intensity of the stable free radicals from the total intensity. The solid line shows the decay curve calculated by eq 1: the values of A and B are 1.3 $\times$ 10^{-2} and 1.1 $\times$ 10^{-4}, respectively.

of stable radicals decreases with an increase in temperature. This experimental fact reflects that matrices which trap free radicals have the heterogeneity in structure. The heterogeneity can be represented as the degree of disorder of molecular orientation, on which the reactivity of free radicals depends. For instance, more ordered the local structure is, more stable the free radicals are. The free radicals trapped in the region of more ordered structure over a critical degree should be stable. The reduced fractional amounts of free radicals, calculated by subtracting spectral intensity of the stable free radicals from the total intensity, are plotted against storage time, as shown in Figure 4. When the logarithms of the fractional amount and the inverse amount were plotted against time, the plotted points in both cases show the obvious deviation from the linear plots. From these facts, the kinetics of the decay cannot be explained by both treatments of the first- and second-order reactions. Then, the analysis of the data of the decay reaction was made on the basis of three-dimensional diffusion-controlled reaction theory. The theory deals with the bimolecular reaction whose rate constant is dependent on time as a result of, for example, molecular diffusions. The following Waite's equation[24,25] concerning the diffusion-controlled bimolecular reaction was applied.

$$C_0/C = 1 + 8\pi r_0 D C_0 (1 + 2^{1/2} r_0/(\pi D t)^{1/2}) t$$
$$= 1 + A(t)^{1/2} + Bt \qquad (1)$$

where

$$A = 8{\cdot}2^{1/2} r_0{}^2 C_0 (\pi D)^{1/2} \qquad (2)$$

$$B = 8\pi r_0 D C_0 \qquad (3)$$

C_0 is the initial value of radical concentration. D and r_0 are diffusion constant and capture of radius, respectively. The solid line in Figure 4 shows the calculated decay curve obtained by the method of least-squares fitting.

Consequently, the values of A and B in the equation were found to be 1.3 $\times$ 10^{-2} $s^{-0.5}$ and 1.1 $\times$ 10^{-4} s^{-1}, at 403 K, respectively. The values of A and B were obtained to be 6.1 $\times$ 10^{-3} $s^{-0.5}$ and 8.3 $\times$ 10^{-5} s^{-1} at 373 K, respectively, in the same manner. The exact values at higher temperatures could not be estimated because of the rapid reaction. The simulated curve is in good agreement with data based on diffusion-controlled reaction theory and makes for improved interpretation of the decay reaction of the free radicals trapped in solid polymer. The value of $1/A^2$ indicates a good measure of time constant, τ, of the decay reaction. The second term, $At^{1/2}$, should be important in eq 1 in the short range of storage time. Eventually, the value of A^2 corresponds to frequency, f, of molecular motion. The values of A^2 were plotted against the reciprocal absolute temperature in the so-called transition map by arranged by Wada,[26] as shown in Figure 5. The map indicated the relation between the time constant and temperature. The frequency of the decay reaction was found to fall close to the frequency for molecular motion associated with α-dispersion on the transition map. Dynamic mechanical relaxation behaviors of poly(tetrafluoroethylene) (PTFE) have been studied by many investigators. γ, β', β, and α relaxation modes were found around 170, 260, 320, and 400 K, respectively.[27] γ and β' relaxation modes were associated with local mode and micro-Brownian motion in the amorphous region. β relaxation[28,29] was related with crystalline phase transitions of helical conformation, and α relaxation[30] was associated with a rotation of a PTFE chain like a rod (rod-type rotation) in the paracrystalline region (intermediate phase), which was clarified by the NMR studies.[31,32] These results in the present study conclude that the decay reaction of free radicals in PTFE is mainly due to the molecular motion in the paracrystalline region.

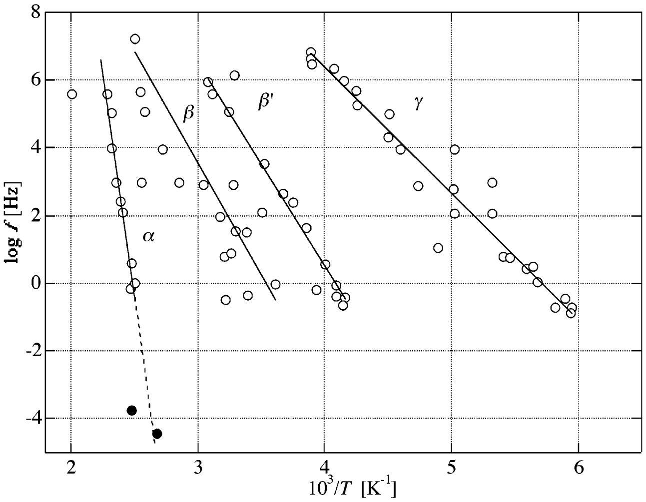

Figure 5. Comparison of the time constants for the decay reaction of free radicals (●) with those for molecular motion of PTFE matrix (○). Solid lines and open symbols are the reference data.[26]

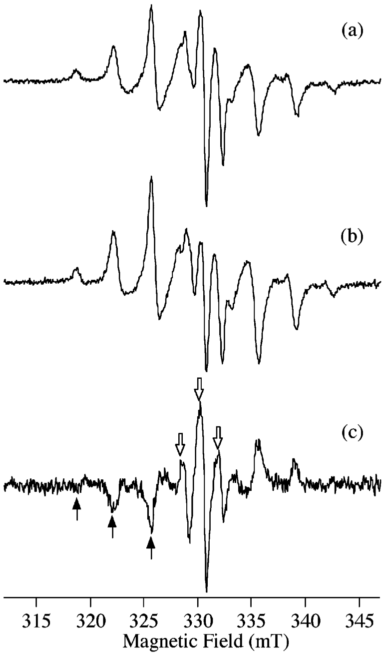

Figure 6. Change of ESR spectra of free radicals trapped in γ-irradiated NCL PTFE before (b) and after (a) heat treatment at 383 K. Measurements were carried out at room temperature. Spectrum c was obtained by the subtraction spectrum b from spectrum a. The characteristic peaks indicated by arrows are in spectrum c originated from the main chain alkyl type ($M^{\bullet}$) (filled arrows) and chain end alkyl type ($E^{\bullet}$) (open arrows) radicals.

β-Scission Reaction of Main Chain Radicals ($M^{\bullet}$). The decay reaction was interpreted in terms of diffusion-controlled reaction theory. The next question is, what diffuses in PTFE matrices? The translation diffusion of the segments never occurs in the paracrystalline region at extremely lower temperatures than the melting one. The free radical migration[30] in the region is now discussed. Figure 6 shows the change of ESR spectrum of NCL PTFE with heat treatment at 383 K for 5 min. The spectrum before the heat treatment was subtracted from one after heat treatment. The difference spectrum is shown in Figure 6c, where the phase of the 2 × 5 lines spectrum marked with filled arrows is opposite to that of the 3 × 3 lines marked with open arrows. These

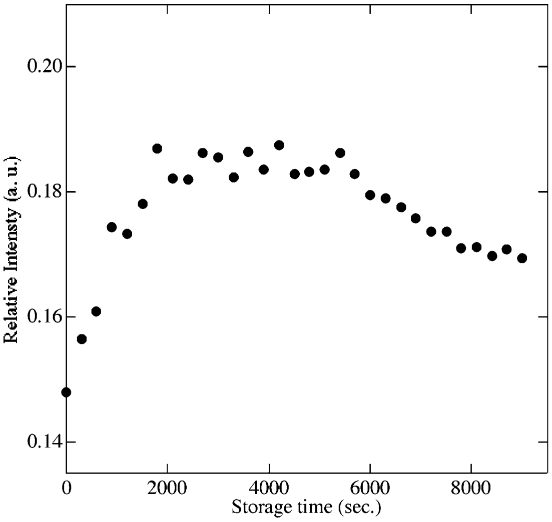

Figure 7. Change of mole fraction of chain end free radicals with storage time at 353 K. The mole fraction was calculated by the double integration of the $E^{\bullet}$ and $M^{\bullet}$ spectra after the deconvolution.

results indicate that the 3 × 3 lines spectrum from the chain end radicals ($E^{\bullet}$) increases, whereas the 2 × 5 lines one from the main chain radicals ($M^{\bullet}$) decreases during the heat treatment. This conversion of $M^{\bullet}$ to $E^{\bullet}$ suggests that the following β-scission reaction occurs.

$$-CF_2-C^{\bullet}F-CF_2{-}{-}{-}CF_2-CF_2- \rightarrow -CF_2-CF{=}CF_2 + -CF_2-CF_2^{\bullet} \quad (4)$$

The repetitions of the β-scission reaction and fluorine atom abstraction of $E^{\bullet}$ from the neighbor chain follow the decay reaction of free radicals and/or the movement of $M^{\bullet}$ to the more ordered region.

$$-CF_2-CF_2^{\bullet} + -CF_2-CF_2-CF_2- \rightarrow -CF_2-CF_3 + -CF_2-C^{\bullet}F-CF_2- \quad (5)$$

The $M^{\bullet}$ trapped in the ordered region has a low rate of reaction 4. Figure 7 shows the change of the mole fraction of $E^{\bullet}$ with storage time at 353 K. The mole fraction increases gradually to an asymptotic value and begins to decrease around 6000 s without change of total intensity of the ESR spectrum. The rate of reaction 4, $M^{\bullet} \rightarrow E^{\bullet}$, is larger than that of reaction 5, $E^{\bullet} \rightarrow M^{\bullet}$, for the short duration time. The unstable radicals, $M^{\bullet}$, trapped in the disordered region at 353 K decrease, and the radicals, $E^{\bullet}$, increase gradually. The rate of reaction 4 becomes equal to that of reaction 5, $E^{\bullet} \rightarrow M^{\bullet}$.

Finally, the unstable radicals, $M^{\bullet}$, disappear, and then reaction 5 becomes remarkable. The rates of reactions 4 and 5 change with the temperature of heat treatment. The amounts of $M^{\bullet}$ and $E^{\bullet}$ which give (4) and (5) also change with the temperature.

Fluorine Atom Abstraction of Chain End Radicals ($E^{\bullet}$). Fluorine atom abstraction of chain end radicals ($E^{\bullet}$) from the neighbor chain (5) should take an important role in the diffusion of free radicals, so-called free radical migration. To confirm reaction 5, the variation of the ESR spectrum of chain end radicals ($E^{\bullet}$) was observed with storage time at 403 K. The radicals

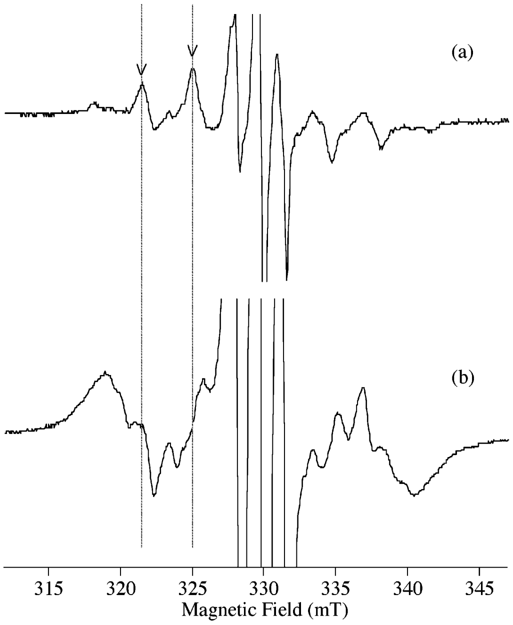

Figure 8. Change of ESR spectra of chain endfree radicals trapped in γ-irradiated CL PTFE before (b) and after (a) heat treatment at 403 K for 660 min. Measurements were carried out at room temperature.

($E^{\bullet}$) are obtained by UV illumination of main chain radicals in a vacuum as mentioned in the Experimental Section. As shown in Figure 8b, the enlarged ESR spectrum after the UV illumination is mainly the 3 × 3 lines assigned to be chain end radicals ($E^{\bullet}$) and does not contain 2 × 5 lines due to main chain radicals ($M^{\bullet}$). For instance, the intensities at the magnetic field indicated by the dotted lines are very weak. Figure 8a shows the enlarged spectrum after heat treatment at 403 K for 660 min. Surprisingly, radicals ($M^{\bullet}$) appear, though ca. half of the free radicals decay. It is confirmed that the intensity of the 2 × 5 lines spectrum indicated by the arrows grows during the heat treatment. This fact suggests that a portion of $E^{\bullet}$ converts to $M^{\bullet}$ and another portion decay at 403 K. Consequently, reactions 4 and 5 repeat and free radicals $M^{\bullet}$ and $E^{\bullet}$ encounter and couple each other in several manners. For example, T type cross-linking are formed by coupling of $M^{\bullet}$ and $E^{\bullet}$. Fluorine abstraction of $M^{\bullet}$ from the neighbor chain can be also considered. Anyhow, the unstable radicals at temperatures give rise to several reactions, a portion of the radicals decays, and another portion moves to the region where the radicals are stable, finally. The rates of the reactions have strong effects on the polymer structure of much heterogeneity. The heterogeneity of molecular mobility of free radicals is published in a forthcoming paper.

4. Conclusions

Several reactions in solid PTFE polymer were detected directly:

1. β-Scission reaction of main chain radicals.

$$-\mathrm{CF_2}-\mathrm{C^{\bullet}F}-\mathrm{CF_2}\text{---}\,\mathrm{CF_2}-\mathrm{CF_2}- \rightarrow -\mathrm{CF_2}-\mathrm{CF{=}CF_2} + -\mathrm{CF_2}-\mathrm{CF_2^{\bullet}} \quad (4)$$

2. Fluorine abstraction of chain end radicals.

$$-\mathrm{CF_2}-\mathrm{CF_2^{\bullet}} + -\mathrm{CF_2}-\mathrm{CF_2}-\mathrm{CF_2}- \rightarrow -\mathrm{CF_2}-\mathrm{CF_3} + -\mathrm{CF_2}-\mathrm{C^{\bullet}F}-\mathrm{CF_2}- \quad (5)$$

3. The decay reaction of free radicals by the repetitions of (4) and (5).

Fluorine abstraction of main chain radicals may join the decay reaction. The decay reaction at a temperature was analyzed on the basis of diffusion-controlled theory and closely related with molecular motion in the paracrystalline region, associated with α-relaxation of PTFE. The unstable free radicals in the temperature increase with an increase in temperature. The rates of the β-scission reaction and the fluorine abstraction decrease and increase, respectively, with storage time at a temperature. The behavior depends on the temperature of the heat treatment. These results reflect much heterogeneity in the polymer structure of PTFE. The rate of the decay reaction in cross-linked PTFE is larger than the non-cross-linked PTFE. The free radicals in the non-cross-linked PTFE are trapped in the disordered region made by the cross-linking.

References and Notes

(1) Shimada, S. *Prog. Polym. Sci.* **1992**, *17*, 1045.
(2) Shimada, S.; Kashiwabara, H. *Polym. J.* **1974**, *6*, 448.
(3) Shimada, S.; Maeda, M.; Hori, Y.; Kashiwabara, H. *Polymer* **1977**, *18*, 19.
(4) Shimada, S.; Hori, Y.; Kashiwabara, H. *Polymer* **1977**, *18*, 25.
(5) Shimada, S.; Hori, Y.; Kashiwabara, H. *Polymer* **1981**, *22*, 1377.
(6) Shimada, S.; Hori, Y.; Kashiwabara, H. *Macromolecules* **1988**, *21*, 979.
(7) Seguchi, T.; Tamura, N. *J. Polym. Sci., Polym. Chem.* **1974**, *12*, 181.
(8) Shimada, S.; Hori, Y.; Kashiwabara, H. *Polymer* **1977**, *18*, 151.
(9) Hori, Y.; Shimada, S.; Kashiwabara, H. *Polymer* **1979**, *20*, 181.
(10) Rexroad, H. N.; Gordy, W. *J. Chem. Phys.* **1959**, *30*, 399.
(11) Matsugasita, T.; Shinohara, K. *J. Chem. Phys.* **1961**, *35*, 1652.
(12) Tamura, N. *J. Chem. Phys.* **1962**, *37*, 479.
(13) Iwasaki, M.; Sakai, Y. *J. Polym. Sci., Part A-2* **1968**, *6*, 365.
(14) Moriuchi, S.; Nakamura, M.; Shimada, S.; Kashiwabara, H.; Sohma, J. *Polymer* **1970**, *11*, 630.
(15) Toriyama, K.; Iwasaki, M. *J. Chem. Phys.* **1969**, *73*, 2919.
(16) Siegel, S.; Hedgoeth, H. *J. Chem. Phys.* **1967**, *46*, 3904.
(17) Tutiya, M. *J. Appl. Phys.* **1972**, *11*, 1542.
(18) Sun, J.; Zhang, Y.; Zhong, X. *Polym. Commun.* **1994**, *35*, 2881.
(19) Oshima, A.; Tabata, Y.; Kudoh, H.; Seguchi, T. *Radiat. Phys. Chem.* **1995**, *45*, 269.
(20) Tabata, Y.; Oshima, A.; Takashika, K.; Seguchi, T. *Radiat. Phys. Chem.* **1996**, *48*, 563.
(21) Oshima, A.; Ikeda, S.; Seguchi, T.; Tabata, Y. *Radiat. Phys. Chem.* **1997**, *49*, 279.
(22) Oshima, A.; Seguchi, T.; Tabata, Y. *Radiat. Phys. Chem.* **1997**, *50*, 601.
(23) Oshima, A.; Seguchi, T.; Tabata, Y. *Radiat. Phys. Chem.* **1999**, *55*, 61.
(24) Waite, T. R. *J. Chem. Phys.* **1960**, *32*, 21.
(25) Waite, T. R. *Phys. Rev.* **1957**, *107*, 463.
(26) Wada, Y. *J. Phys. Soc. Jpn.* **1961**, *16*, 1226.
(27) McCrum, N. G. *J. Polym. Sci.* **1959**, *34*, 35.
(28) Hyndman, D.; Origlio, G. F. *J. Appl. Phys.* **1960**, *31*, 1849.
(29) Tuge, K.; Wada, Y. *Jpn. Appl. Phys.* **1962**, *1*, 2701.
(30) Iwayanagi, S.; Sakurai, I. *J. Polym. Sci.* **1966**, *C15*, 29.
(31)] Iwayanagi, S.; Sakurai, I. *Rep. Prog. Polym. Phys. Jpn.* **1962**, *5*, 222.
(32) Ohzawa, Y.; Wada, Y. *Jpn. Appl. Phys.* **1962**, *3*, 436.
(33) Shimada, S.; Kashiwabara, H.; Sohma, J. *J. Polym. Sci., Part A-2* **1970**, *8*, 1291.

MA030206V